



Enhanced Dictionary based Sparse Representation Fusion for Multi-temporal Remote Sensing Images

Anisha M. Lal & S. Margret Anoucia

To cite this article: Anisha M. Lal & S. Margret Anoucia (2016) Enhanced Dictionary based Sparse Representation Fusion for Multi-temporal Remote Sensing Images, European Journal of Remote Sensing, 49:1, 317-336, DOI: [10.5721/EuJRS20164918](https://doi.org/10.5721/EuJRS20164918)

To link to this article: <http://dx.doi.org/10.5721/EuJRS20164918>



© 2016 The Author(s). Published by Taylor & Francis.



Published online: 17 Feb 2017.



Submit your article to this journal [↗](#)



Article views: 82



View related articles [↗](#)



View Crossmark data [↗](#)



Enhanced Dictionary based Sparse Representation Fusion for Multi-temporal Remote Sensing Images

Anisha M. Lal* and S. Margret Anuncia

SCOPE, VIT University, Vellore, 632014, India

*Corresponding author, e-mail address: anishamlal@vit.ac.in

Abstract

In remote sensing, image fusion is the process of blending two images to obtain finer details of the fused image. In this paper, an enhanced dictionary-based sparse representation (EDSR) is proposed for multitemporal image fusion. Multitemporal remote satellite images acquired on the same geographical area at different acquisition dates are merged to obtain a fused image for further analysis. Sparse representation of the image is employed in the approximation and representation of the target image. In order to improve the performance of the fusion process, a locally adaptive dictionary is created such that the dictionary contains patches extracted from both source images. The reconstruction of the image is performed using maximum absolute coefficients through the learned dictionary. The proposed EDSR technique has been compared quantitatively and qualitatively with the existing techniques, such as PCA, DWT, SWT, Ehlers, and sparse representation (SR), to evaluate its performance. The EDSR performs well in mutual information (MI) with 3.4742 and feature mutual information (FMI) with 0.4790 and provides better results in the case of degree of distortion, UIQI, and ERGAS for dataset 1 than the existing fusion methods. Experimental results on LANDSAT images revealed that the proposed technique is more effective in terms of preservation of spectral information, errors, color, and visual quality of the fused product.

Keywords: Sparse representation, multitemporal, image fusion, remote sensing.

Introduction

Nowadays, multitemporal images are widely used in various fields such as remote sensing and computer vision for fusion and further analysis of the fused image. Image fusion is the process of blending two or more images from a particular viewpoint into a single fused image that is more enlightening for computation and surveillance. The process of image fusion is to generate a composite image by fusing the corresponding information from both the source images of the same geographic location. In an image fusion system, the input multitemporal images can be acquired from different sensors or from sensors whose optical parameters are changed and the obtained fused image can be interpreted easily than a single image and will be more suitable for human and machine perception. Over the last decade,

image fusion has found enormous applications in the area of remote sensing.

In this paper, a proposed method of enhanced dictionary-based sparse fusion for multitemporal remote sensing images is carried out, which can be used for further analysis. The main objective of this paper is to design an image fusion method based on sparse representation for multitemporal multispectral remote sensing images which highlights the finer details in the images. The proposed method is mainly focused on multitemporal images which improve the effectiveness and robustness of the process. Compared with the existing techniques, the following novelties have been achieved: First, the regularization parameter q adopted in the proposed technique is adaptive. Second, updating the dictionary is also done at each step. And third, updating the dictionary leads to speeding up the process of sparse decomposition and improves the effectiveness and robustness of remote sensing image fusion. In addition, the proposed method will be thoroughly evaluated against the state-of-the-art.

This paper is organized as follows. Section “Sparse representation” gives a brief review of the theory of sparse representation. Section “Related work” presents an overview of the related works carried out so far. The proposed technique is presented in detail in Section “Proposed Enhanced Dictionary-based Sparse Representation (EDSR)”. In Section “Experimental results and discussion” experimental results and discussion are discussed. Performance evaluation of the results for image fusion are analyzed in Section “Performance evaluation”. Finally, Section “Conclusion and future works” draws the conclusions of this work.

Sparse representation

Sparse representation is a dominant tool for labelling signals. Recently, sparse representation plays a major role in image processing in various applications such as remote sensing images and medical imaging. In sparse representation, a learned dictionary is used for the approximation of the signals. A dictionary is a collection of prototype signals (atoms) formulated as column vectors of a predefined length. The dictionary D of K atoms can be represented as a matrix of size $m \times K$, such that $D \in R^{m \times K}$. Each column is a basic atom of the dictionary, and K stands for the total number of atoms in D . When $m < K$, the dictionary is referred to as an overcomplete dictionary. In this implication, each signal is approximated as a linear combination of a few atoms from the dictionary D . Representation of signal or image X can be written as:

$$X = DS \quad [1]$$

where S is a vector that contains representation coefficients of the signal X , provided that S has the fewest nonzero entries such that $S \in R^K$ and $X \in R^m$. The main idea here is to find the learning dictionary D and sparse vector S . In this type of problem, the dictionary needs to be created such that its content can be used as a training set in the reconstruction of the target image. That is to say, for each approximation, there should be a small number of nonzero coefficients. The optimization problem in Equation [1] can be represented as:

$$\|X - DS\|_j \leq q \quad [2]$$

where $\|X - DS\|_j$ is the approximated error of the input image and j is the deviation l -norms, which can be 0, 1, . . . , ∞ . When $j=0$, the sparse vector has a minimum number of nonzero elements and the approximation of X becomes:

$$X = \arg \min \|S\|_0 \text{ such that } X = DS \quad [3]$$

where $\|S\|_0$ signifies the number of nonzero elements of S . Solving Equation [3] is nondeterministic polynomial-time hard (NP-hard) in general. Several relaxation strategies are developed for approximating the solution of Equation [3], such as basis pursuit [Ahron, 2006], focal underdetermined system solver [Knee, 2012], and OMP [Tropp and Anna, 2007]. The choice of dictionary plays an important role in sparse representation. An approach applies the learning techniques to infer the dictionary from the training set, which is studied widely at present, such as the method of optimal directions [Bach et al., 2010] and K-SVD [Aharon et al., 2006]. The learned dictionary from the training set exhibits better performance in specific applications.

Related work

The area of remote sensing image fusion has attracted the attention of many researchers in recent years. Several image fusion methods have been devised and applied to various applications. The common methods used for fusion are principal component analysis (PCA) [Lal and Margret, 2015a], intensity hue saturation (IHS), wavelet transform (WT) [Lal and Margret, 2015a], Laplacian pyramid (LP), Bayesian, Brovey transform (BT), and maximum entropy [Wang et al., 2005]. Sparse representation was first introduced in image fusion by Yang and Shutao [2010], and since then, it has become a renowned image fusion technique amongst all other techniques. This technique presumes that the sparse property exists in the image data such that the data can be represented in a different manner.

In remote sensing, the sparse representation method has been fine-tuned into different aspects in order to produce more realistic fusion results. In a recent work [Wei et al., 2015], the authors utilized sparse regularization constraint in fusing multispectral and hyperspectral images. The atoms of the training dictionary were obtained from the input images, and the image patches formed as a linear combination of that dictionary. And online dictionary learning was used to optimize the problem. He et al. [2014] applied regularization control based on the spatial and spectral characteristics of panchromatic and multispectral images recorded by different sensors deployed in the same area or scene. The method also uses both spatial and spectral sparsity priors for image fusion. Moreover, their method utilizes limited patch atoms extracted from input images for the learned dictionary. Optimization of the fusion process is done using two parameters that are enforced on the total variation (TV) seminorm. One parameter is based on linear regression (LR) and another based on principal component pursuit (PCP).

Another improved version of the sparse method proposed is by Liu et al. [2014], where the registered images are decomposed into multiple scales prior to the fusion process.

The decomposed images are then sparse coded and eventually reconstructed using the inverse process to get the resultant image. Decomposition of sparse coefficients from the matrix of input multispectral and panchromatic images has also been reported by Yu et al. [2014]. As the values of higher coefficients of the panchromatic image are set to 0, the combined and balanced coefficients are directly used for fusion of the higher resolution and lower resolution images. Fusion is accomplished by using image patches from a learned dictionary created using the discrete curvelet transform (DCT) method. Zhu and Richard [2013] proposed a pansharpening sparse method for fusion of satellite images obtained at the same time and location. Their method makes use of two types of training dictionaries. One dictionary consists of patches from a higher spatial resolution image while the other contains patches from a lower-resolution down-sampled image. Sparse coding uses both L_1 and L_2 norms to obtain sparse coefficients, and the fusion is done by blending coefficients from both input images. Pansharpening sparse fusion can also be implemented by infusing missing image details [Vicinanza et al., 2015]. The authors used two separate dictionaries, one for each image type. Moreover, image filtering is done through two modulation transfer functions (MTF), and the missing spatial details are inserted only in the higher multispectral image during the reconstruction phase. In another article by Huang and Huihui [2012], the uses of two separate sparse-oriented training dictionaries have been anticipated. A higher-resolution image and a lower-resolution image acquired at different time intervals are used to extract atoms of the dictionary. All the dictionaries and grouping coefficients are updated in turn, while other parameters are set fixed. Iqbal et al. [2012] offered a version of sparse representation that focuses on the best basis sparse vectors' higher-resolution and lower-resolution image fusion. An image that has a lower resolution is boosted to match the counter higher-resolution image in the combining process. The studies discussed in this section have shown extensive exploration of sparse-based methods. However, although the SR algorithm has been reported to have a relatively good performance, there is still a need for improvement in the dictionary creation [Vicinanza et al., 2015]. Furthermore, it has been found that most of the existing image fusion algorithms have high computational cost when it comes to data decomposition [Wei et al., 2015]. This shows the necessity to further investigate this algorithm. This work aims to address the aforementioned challenges.

Proposed Enhanced Dictionary-based Sparse Representation (EDSR)

The proposed enhanced dictionary-based sparse representation (EDSR) is mainly used for multitemporal images in remote sensing applications. The proposed framework for multitemporal image fusion is shown in Figure 1.

Two Landsat images acquired at different timings, T1 and T2, are considered for the analysis of multitemporal image fusion. Images acquired from a satellite might have some noise because of the electronics inside the sensors, atmospheric condition, and registration or transmission errors [Pohl, 2014]. Before the images are processed, each image is filtered using a Gaussian low-pass filter to remove unwanted noise which could affect the final result of the fusion process and to enhance the image. The preprocessed images are then subjected to fusion using the enhanced dictionary-based sparse representation.

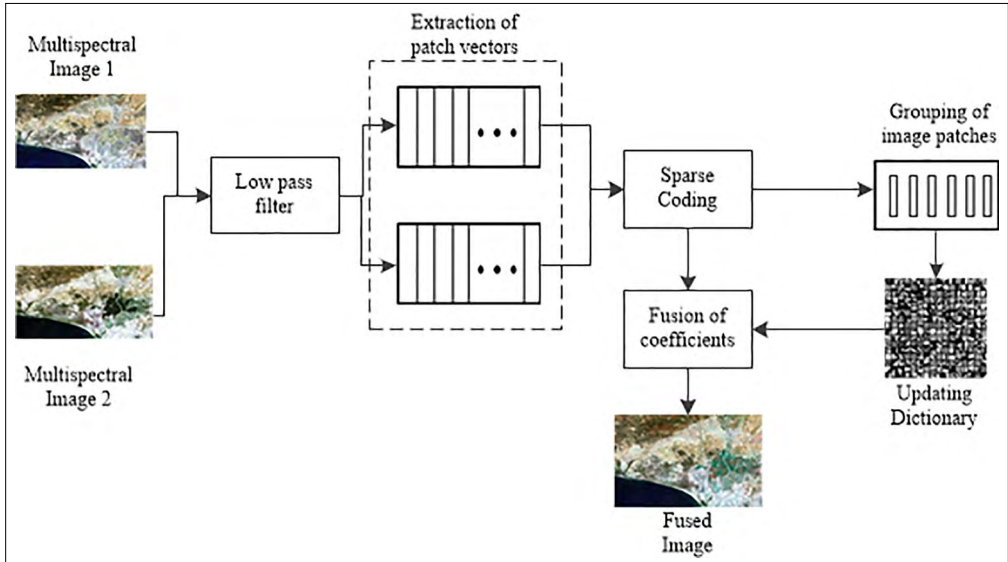


Figure 1 - Proposed framework of EDSR for multi-temporal image fusion.

The training image patches are extracted from both preprocessed images using an operator R . Extracting the image patch x from the observed image X can be represented as:

$$x_j = R_j(X) \quad [4]$$

where $R_j(\cdot)$ is an operator that extracts the patch x_j from location (j) in the image X . To put back the patch x_j in the j position, transpose $R_j^T(\cdot)$ is used during the image reconstruction phase. Since very small image patches lose the compactness of the dictionary and very large patches affect the multispectral features of the image, here, the size of the image patches is determined to be $\sqrt{64} \times \sqrt{64}$. Each extracted patch is localized by subtracting its mean value and converting it into a column vector as the process produce vectors v_1 to v_j , where j is the index of the last vector. Thereafter, the vectors of the patches from an image X are combined into a matrix V . The same process is done for each preprocessed image. The matrix obtained from this stage is required for process searching for the best basis vectors in sparse coding.

An estimation of relevant sparse vectors is conducted, which determines how the signals should be sparsely represented. This unsupervised learning process is referred to as sparse coding. It is an essential part of the sparse representation method, which is designed to automatically discover the best basis vectors using unlabeled data. Sparse coding attempts to solve the problem in Equation [3], which can be rewritten as:

$$\min \|X - DS\| \quad j \leq q \text{ such that } \|S\|_0 \leq q \quad [5]$$

Even though there are several sparse coding techniques, such as basis pursuit (BP), matching

pursuit (MP), FOCUSS, and others, we opt for orthogonal matching pursuit (OMP) because it is more efficient. Likewise, for the rationale of further upgrading sparse coding, we do adopt an enhanced version of sparse coding known as improved sparse coding (ISC). This version of sparse coding introduces the lower bound of the errors in signals as proposed in Lu et al. [2011]. With regard to the upper and lower bounds, Equation [5] now becomes:

$$\min \|X - DS\|_2^2 \leq q \text{ such that } p \leq \|S\|_2^2 \leq q \quad [6]$$

where p is the lower bound of the sparse regularization term. The problem is the NP-hard sparse decomposition because of \mathbf{l}_0 -norm, but it can be approximated by \mathbf{l}_1 -norm as long as the coefficients are still sparse. This problem can be solved by the OMP algorithm [Tropp and Anna, 2007; Lal et al., 2015b], which is commonly found in the K-SVD package. In K-SVD [Aharon et al., 2006], the dictionary is initialized with the extracted image patches. Then the patches are used to perform sparse coding and update the dictionary.

OMP Algorithm

The OMP method to compute sparse coefficients for each image:

$$S = \min_{\alpha \in \mathbb{R}^m} \frac{1}{2} \|X - DS\|_2^2 \text{ such that } \|S\|_0 \leq q$$

Step 1: Initialization: $\alpha=0$, residual $r=x$, active set $\Omega=\emptyset$;

Step 2: While $\|\alpha\|_0 < L$;

{
Select the element with maximum correlation with the residual

$$\hat{i} = \arg \max_{i=1,2,\dots,m} |d_i^T r|$$

Update the active set, coefficients and residual

$$\Omega = \Omega \cup \hat{i}$$

$$S_\Omega = (d_\Omega^T d_\Omega)^{-1} d_\Omega^T r$$

$$r = x - d_\Omega S_\Omega$$

}

The sparse coefficients $S_{i\Omega}$ and $S_{2\Omega}$ are fused together by using the maximum absolute rule and yield the fused sparse coefficient $S_{F\Omega}$. Then the fused vector W_F is computed using the training dictionary-fused sparse coefficient as follows:

$$W_F = D S_{F\Omega} \quad [7]$$

Subsequently, the fused vector W_F is reshaped into a block of 8×8 , and thereafter, the blocks are adjoined into the fused image as illustrated in the proposed algorithm below.

Proposed EDSR algorithm

Input: LANDSAT images A and B at time $T1$ (1984) and $T2$ (2014)

Output: Fused image F

Initialize: Set overlap = 5, dictionary size = 64×256 , $q = \sqrt{(2 \log(\text{size}(D, 2)))}$
patch size = $\sqrt{64} \times \sqrt{64}$

1. Perform Gaussian low pass filter to both LANDSAT images at time $T1$ and $T2$;
2. Use image A to determine 2-dimension grids of the images;
3. Extract image patches from each source images A and B ;
4. Construct dictionary using Improved Sparse Coding (ISC) as follows:

$$D = \min_D \|X - DS\|_2^2 + \lambda \|S\|_1$$

$$\text{such that } p \leq \|S_i\|_2^2 \leq q, i = 1, \dots, K$$

5. Use Orthogonal Matching Pursuit (OMP) method to compute sparse coefficients for each image,

$$S = \min \|S\|_0 \quad \text{such that } \|X - DS\|_2^2 \leq q$$

6. Select only maximum absolute of the fused vectors,

$$S_F^k = S_A^k \quad \text{if } (\|S_A^k\|_1 > \|S_B^k\|_1) \quad \text{other wise, } S_F^k = S_B^k$$

7. Reconstruct fused image as,

$$F = D \circ S = \sum_{k=1}^n R_k^T (DS_k) / \sum_{k=1}^n R_k^T (1_s)$$

8. End.

The proposed EDSR adopts an adaptive regularization parameter q , which is calculated based on the size of the dictionary. ISC is used to construct the dictionary, and OMP is used to compute the sparse coefficients for images A and B . To fuse the images, only the maximum absolute fused vectors are chosen. The fused image is reconstructed by taking the dot product of the dictionary and the sparse coefficient. The EDSR takes advantage of the adaptive regularization parameter and chooses the maximum absolute fused vectors for fusion. Thus, the EDSR performs better than the traditional methods and basic sparse fusion.

Experimental results and discussion

The proposed EDSR technique is compared with the existing image fusion methods-PCA, discrete wavelet transform (DWT), stationary wavelet transform (SWT), Ehlers, and SR-on several pairs of multitemporal images. In order to carry out an experimental analysis aimed at assessing the effectiveness of the proposed approach, we considered two multitemporal datasets corresponding to the geographical areas of Huelva Province in Southern Spain and Istanbul in Turkey. A detailed description of each dataset is given below.

Datasets related to Huelva province in southern Spain and Istanbul in Turkey

The datasets used in this experiment are made up of two multispectral images acquired by the Landsat thematic mapper sensor of the Landsat 5 satellite and Landsat 8 OLI in an area in Huelva Province, Southern Spain, on October 12, 1984, and August 24, 2014, and in the area in Istanbul, Turkey, on June 12, 1984, and October 21, 2014. From the entire available Landsat scene, a section of 512-512 pixels has been selected as the test site.

An experiment was conducted using data acquired by Landsat 5 and Landsat 8 with a resolution of 30 meters. Two multitemporal images were fused by using the proposed EDSR fusion, PCA, SWT, DWT, Ehlers, and SR fusion methods. Original images of Huelva Province acquired in 1984 and 2014 are shown in Figure 2, and fused images are shown in Figures 3 and 4 below. The original images of Istanbul acquired in 1984 and 2014 are shown in Figure 5, and fused images are shown in Figures 6 and 7 below.

The proposed EDSR technique is compared with the existing five techniques: PCA, DWT, SWT, Ehlers, and SR. The fused results are shown in Figures 3, 4, 6, and 7 for two datasets, which clearly indicate that the proposed EDSR fuses better in terms of visual analysis.

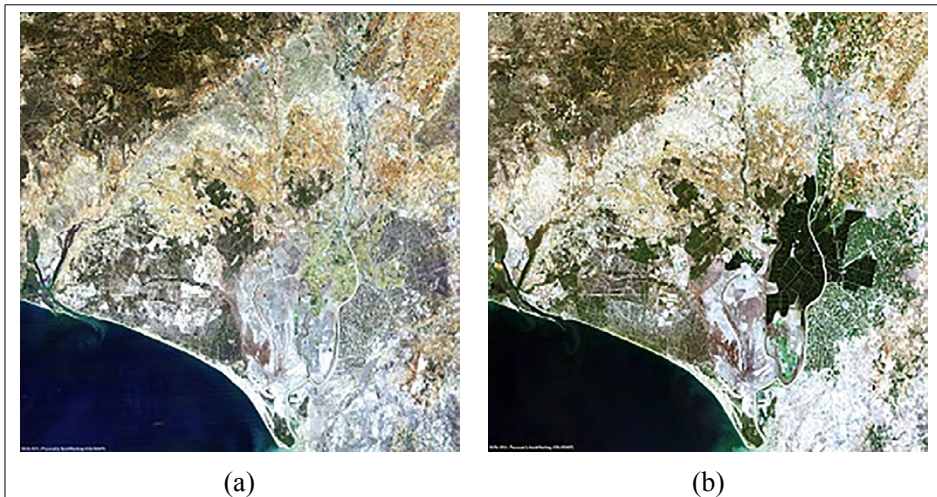


Figure 2 - (a) Original Landsat 5 image recorded on 12 October 1984 from Huelva, Spain. (b) Original Landsat 8 image recorded on 12 August 2014 from Huelva, Spain.

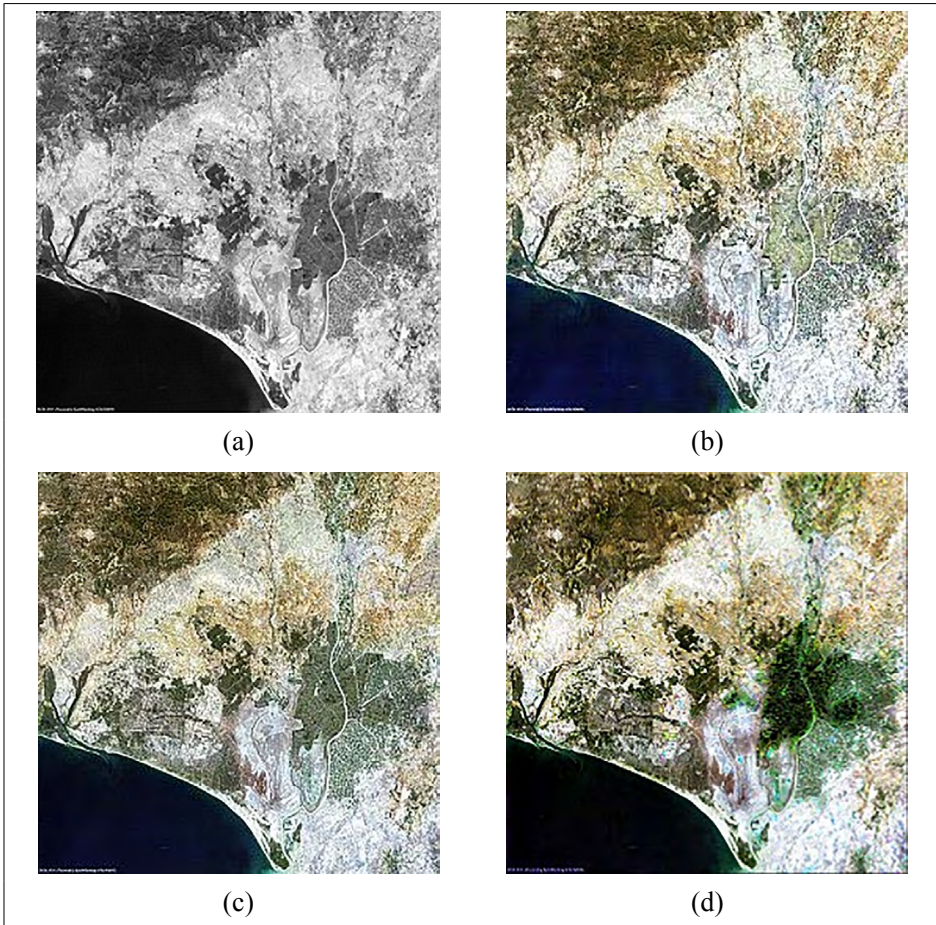


Figure 3 - Fused images. (a) PCA fused image (b) DWT fused image (c) SWT fused image (d) Ehlers fused image.

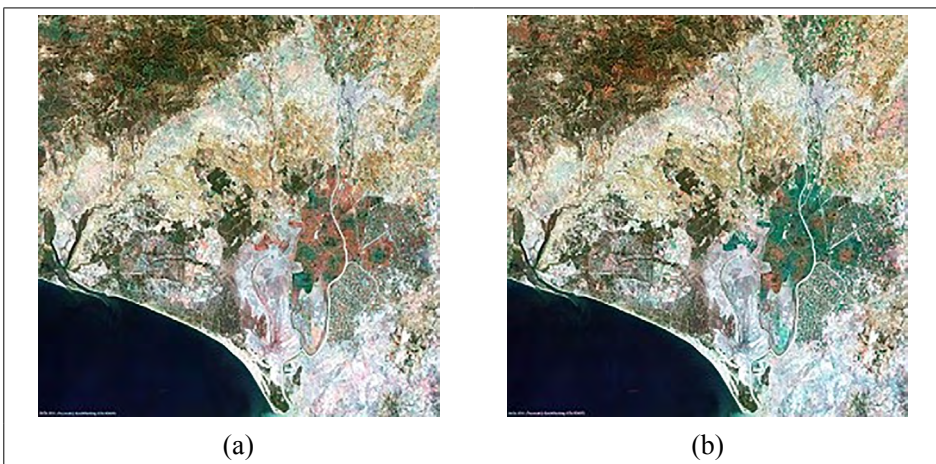


Figure 4 - Fused images. (a) SR fused image (b) EDSR fused image.

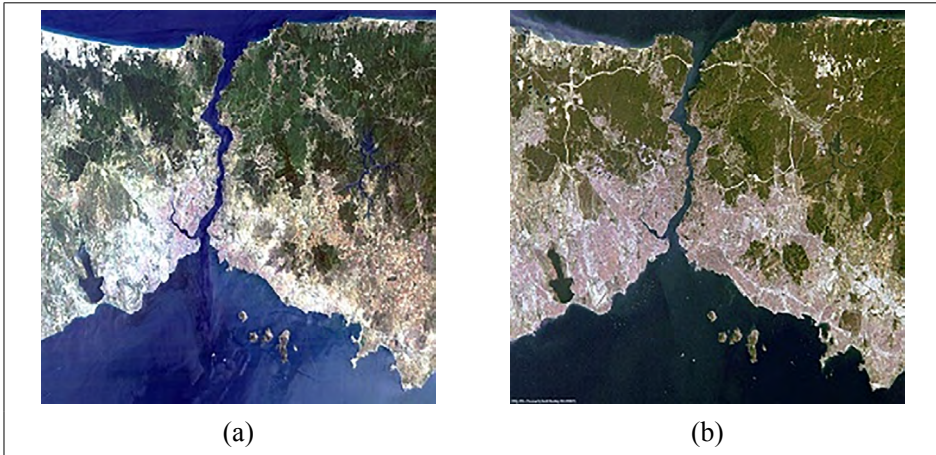


Figure 5 - (a) Original Landsat 5 image recorded on 12 June 1984 from Istanbul, Turkey. (b) Original Landsat 8 image recorded on 21 October 2014 from Istanbul, Turkey.

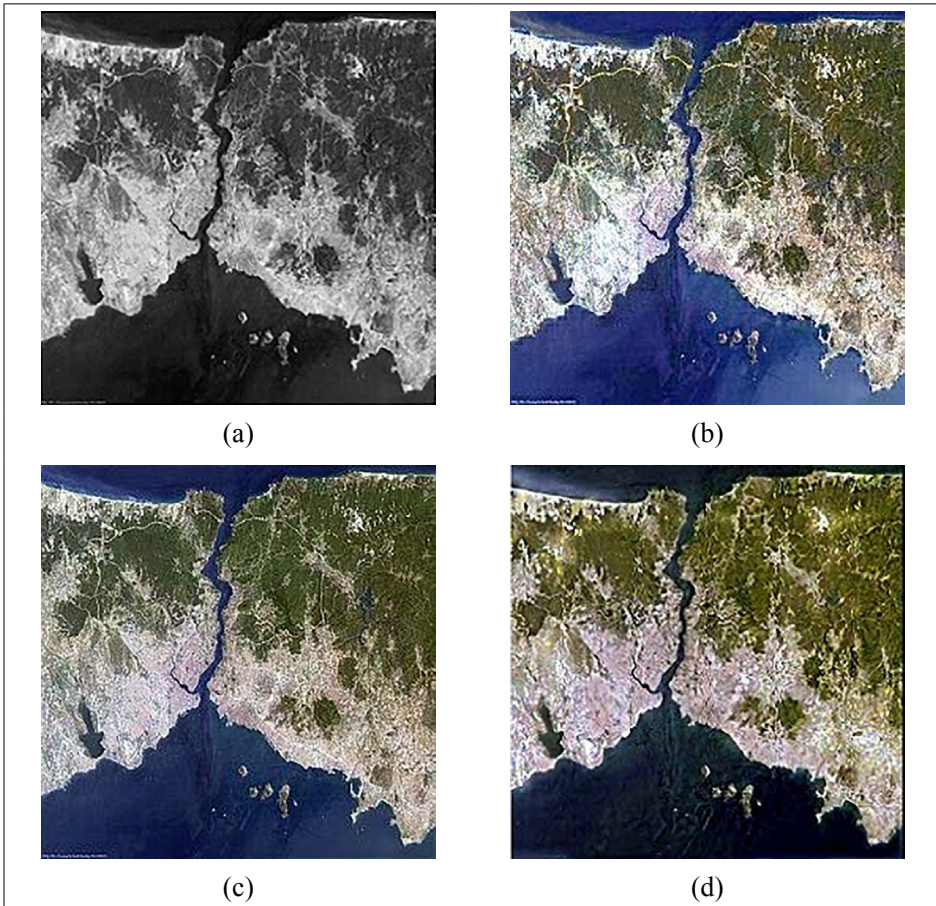


Figure 6 - Fused images. (a) PCA fused image (b) DWT fused image (c) SWT fused image (d) Ehlers fused image.

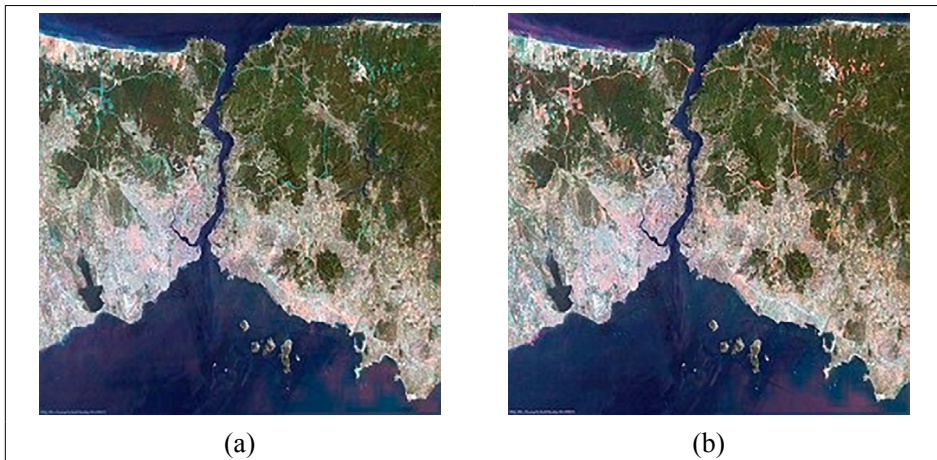


Figure 7 - Fused images. (a) SR fused image (b) EDSR fused image.

Performance evaluation

In this section, the performance evaluation of various methods such as EDSR, SR, SWT, Ehlers, PCA, and DWT are demonstrated based on the results achieved. And the obtained results are associated with qualitative assessments, which are shown in Tables 1 and 2.

The compared results of the images will adopt both objective and subjective assessment criteria that aid in evaluating the quality of the fused image. Objectively, PSNR, RMSE, NCC, SC, NAE, MI, FMI, DD, UIQI, and ERGAS are good criteria in evaluating the difference between the original images and the fused results. Tables 1 and 2 demonstrate the PSNR, RMSE, NCC, SC, NAE, MI, FMI, DD, UIQI, and ERGAS of four different algorithms for two test images. In terms of PSNR, RMSE, NCC, SC, NAE, MI, FMI, DD, UIQI, and ERGAS, the proposed EDSR technique outperforms other existing methods. Subjectively, according to the results of each figure, the proposed technique is able to obtain better visual quality than the existing methods.

Image fusion metrics for evaluation

In order to verify the results obtained through the identified process, simple image metrics were considered to measure the various features of the fused image to get a better depiction of the quality measure. A few assumptions made are found in Sumathi and Barani [2012] and Jagalingam and Hegde [2015].

A and B - the Landsat images at time $T1$ (1984) and $T2$ (2014) of size $m \times n$

F - the fused image to be assessed

i - pixel row index

j - pixel column index

Root Mean Square Error

One obvious way of measuring this similarity is to compute an error signal by subtracting the test signal from the reference and then computing the average energy of the error signal. The root mean square error (RMSE) is the simplest and most widely used full-reference image quality measurement. The RMSE is calculated based on the process given

by Sivasangumani et al. [2014]. Subsequently, PSNR, NCC, SC, and NAE are calculated.

$$RMSE = \sqrt{\frac{1}{mn} \sum_{i=1}^m \sum_{j=1}^n B_{ij} - F_{ij}^2} \quad [8]$$

Peak signal to Noise Ratio

The PSNR computes the peak signal-to-noise ratio, in decibels, between two images. This ratio is used as a quality measurement between the original image and the fused image. The higher the PSNR, the better is the quality of the fused image,

$$PSNR = 10 \times \log_{10} \frac{peak^2}{MSE} \quad [9]$$

where $peak^2$ is the maximum possible pixel value of the image. MSE is the mean square error of the image.

Normalized Cross Correlation

The closeness between two digital images can also be quantified in terms of correlation function. Normalized cross correlation (NK) measures the similarity between two images and is given by the Equation:

$$NCC = \frac{\sum_{i=1}^m \sum_{j=1}^n B_{ij} * F_{ij}}{\sum_{i=1}^m \sum_{j=1}^n (B_{ij})^2} \quad [10]$$

Structural Content

Structural content (SC) is also a correlation-based measure and gauges the similarity between two images. SC is given by the Equation:

$$SC = \frac{\sum_{i=1}^m \sum_{j=1}^n (B_{ij})^2}{\sum_{i=1}^m \sum_{j=1}^n (F_{ij})^2} \quad [11]$$

Normalized Absolute Error

Normalized absolute error (NAE) is the average of the absolute difference between the reference signal and the test image. It is given by the Equation:

$$NAE = \frac{\sum_{i=1}^m \sum_{j=1}^n |B_{ij} - F_{ij}|}{\sum_{i=1}^m \sum_{j=1}^n B_{ij}} \quad [12]$$

Mutual Information

Mutual information [Haghighat et al., 2011] is an image fusion metric that calculates the amount of information conducted from the source images to the fused image. Considering the two source images A and B and the fused image F , the amount of information that F contains about A and B is calculated as:

$$I_{FA}(f;a) = \sum_{f,a} P_{FA}(f,a) \log_2 \frac{P_{FA}(f,a)}{P_F(f).P_A(a)} \quad [13]$$

$$I_{FB}(f;b) = \sum_{f,b} P_{FB}(f,b) \log_2 \frac{P_{FB}(f,b)}{P_F(f).P_B(b)} \quad [14]$$

where $P_{FA}(f,a)$ and $P_{FB}(f,b)$ are the joint probability distributive function of F , A and B . $P_F(f)$ and $P_A(a)$ are the marginal distributive functions of F and A , and $P_F(f)$ and $P_B(b)$ are the marginal distributive functions of F and B , respectively.

Consequently, the image fusion performance measure can be defined as:

$$MI_F^{AB} = I_{FA}(f;a) + I_{FB}(f;b) \quad [15]$$

Feature Mutual Information

Feature mutual information (FMI) [Haghighat and Masoud, 2014] is a nonreference image fusion metric based on mutual information of image features depending on the original images and the fused image. The amount of feature information, which F contains about A and B , is individually measured by means of MI as:

$$I_{FA} = \sum_{f,a} P_{FA}(f,a,z,w) \log_2 \frac{P_{FA}(f,a,z,w)}{P_F(f,a).P_A(z,w)} \quad [16]$$

$$I_{FB} = \sum_{f,b} P_{FB}(f,b,z,w) \log_2 \frac{P_{FB}(f,b,z,w)}{P_F(f,b).P_B(z,w)} \quad [17]$$

where z is the feature used and w is the sliding window of size 3. Eventually, the FMI metric is:

$$FMI_F^{AB} = I_{FA} + I_{FB} \quad [18]$$

Degree of Distortion (DD)

The degree of distortion [Zhu and Richard, 2013] directly reflects the level of fused image distortion. It is evaluated using the Equation below:

$$D = \frac{1}{mn} \sum_{i=1}^m \sum_{j=1}^n |B_{ij} - F_{ij}| \quad [19]$$

The distortion of the fused image is small, whereas the value of D is small.

UIQI (Q-Average)

The UIQI is used to assess the quality of image sharpening. It is evaluated using the mean values and the standard deviations of the original image and the fused image. It is given in the Equation:

$$Q = \frac{\sigma_{AF}}{\sigma_A \sigma_F} \cdot \frac{2\mu_A \mu_F}{(\mu_A^2 + \mu_F^2)} \cdot \frac{2\sigma_A \sigma_F}{(\sigma_A^2 + \sigma_F^2)} \quad [20]$$

where μ_A , σ_A , and μ_F , σ_F are the mean values and standard deviations of the original image A and the fused image F .

ERGAS

The ERGAS reflects the overall quality of the fused image. It represents the difference between the fused image and the original images. It is expressed in the Equation:

$$ERGAS = 100 \frac{k}{l} \sqrt{\frac{1}{n} \sum_{n=1}^N \left[\frac{RMSE_n}{\mu_{Fn}} \right]^2} \quad [21]$$

where $\frac{k}{l}$ is the ratio between the pixel sizes of the fused image and the original images, and $RMSE_n$ and μ_{Fn} are the RMSE and the mean values of the n th band, respectively.

Table 1 - Performance of different methods on source images acquired over Huelva, Spain.

Method	RMSE	PSNR	MI	FMI	NCC	SC	NAE	DD	UIQI	ERGAS
PCA	32.59	17.87	2.33	0.20	0.96	1.03	0.18	9.63	0.65	7.13
DWT	29.11	18.23	3.02	0.40	1.05	0.88	0.16	7.53	0.69	6.45
SWT	29.01	29.01	3.06	0.42	0.98	1.01	0.13	7.43	0.71	5.78
Ehlers	32.80	17.81	2.61	0.34	0.96	1.02	0.18	9.01	0.66	5.23
SR	24.63	20.30	3.45	0.47	0.98	1.02	0.13	6.11	0.87	4.88
EDSR	20.40	21.94	3.47	0.48	0.98	1.03	0.11	5.8	0.89	4.45

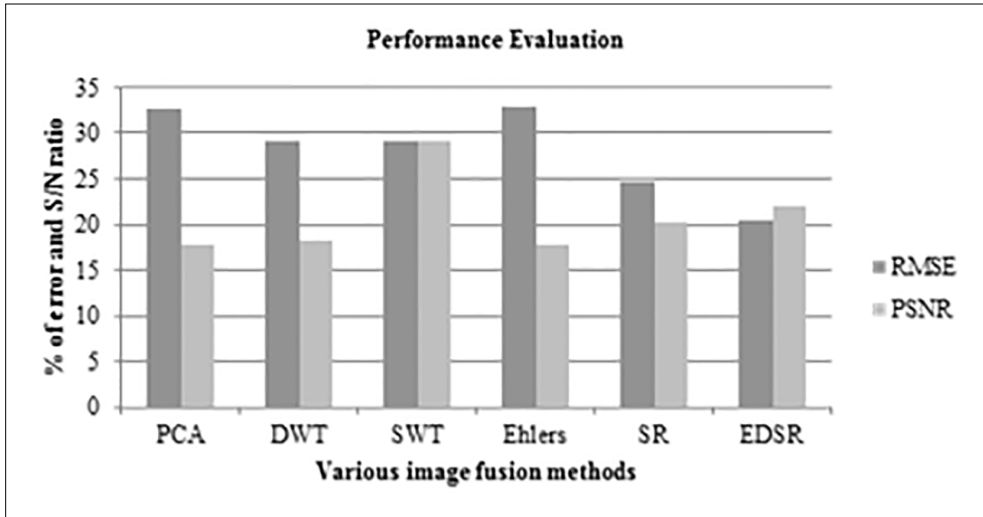


Figure 8 - Performance Evaluation with respect to RMSE and PSNR for dataset 1.

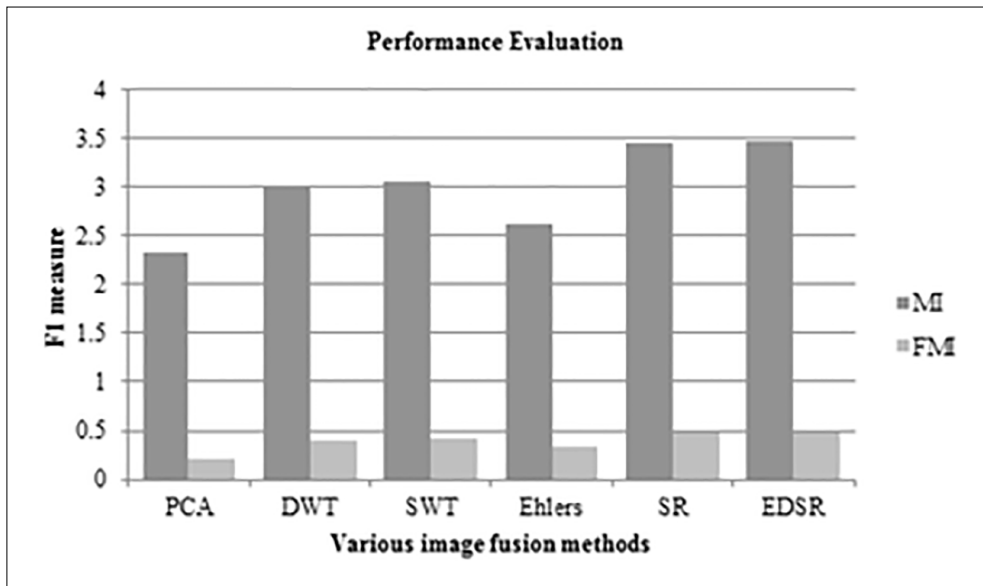


Figure 9 - Performance Evaluation with respect to MI and FMI for dataset 1.

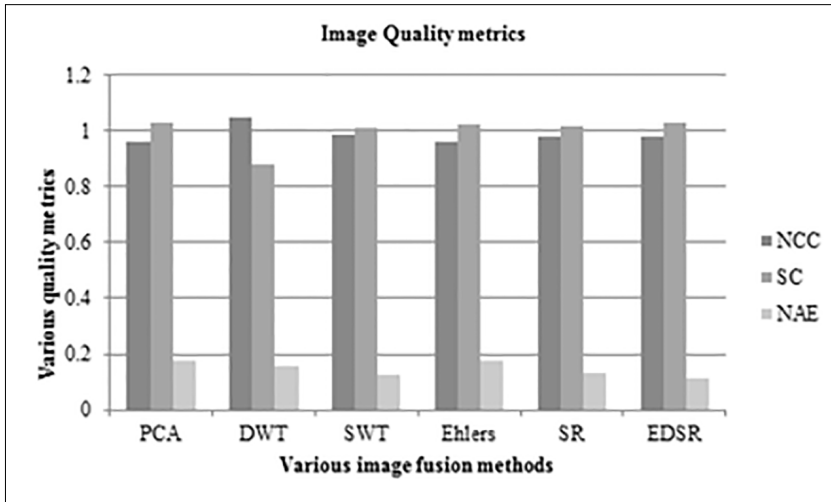


Figure 10 - Various image quality metrics for dataset 1.

Table 2 - Performance of different methods on source images acquired over Istanbul, Turkey.

Method	RMSE	PSNR	MI	FMI	NCC	SC	NAE	DD	UIQI	ERGAS
PCA	27.97	19.20	2.39	0.26	0.99	0.97	0.20	9.32	0.69	7.01
DWT	33.12	17.73	2.90	0.34	1.13	0.74	0.25	7.47	0.7	6.44
SWT	22.45	21.10	2.83	0.35	1.04	0.90	0.17	7.15	0.77	5.32
Ehlers	39.33	16.24	1.70	0.13	0.98	0.92	0.28	9.12	0.65	5.12
SR	20.36	20.96	3.07	0.31	1.03	0.92	0.16	6.01	0.88	4.77
EDSR	20.19	21.20	2.58	0.40	1.03	0.91	0.15	5.71	0.90	4.12

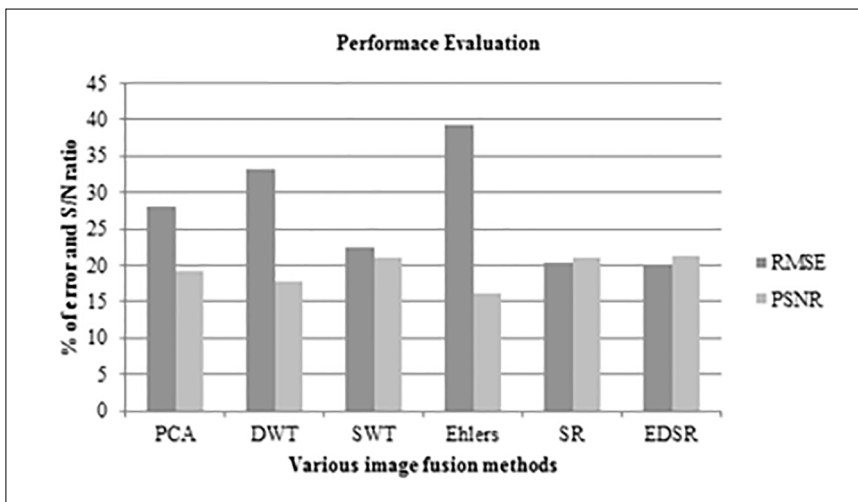


Figure 11 - Performance Evaluation with respect to RMSE and PSNR for dataset 2.

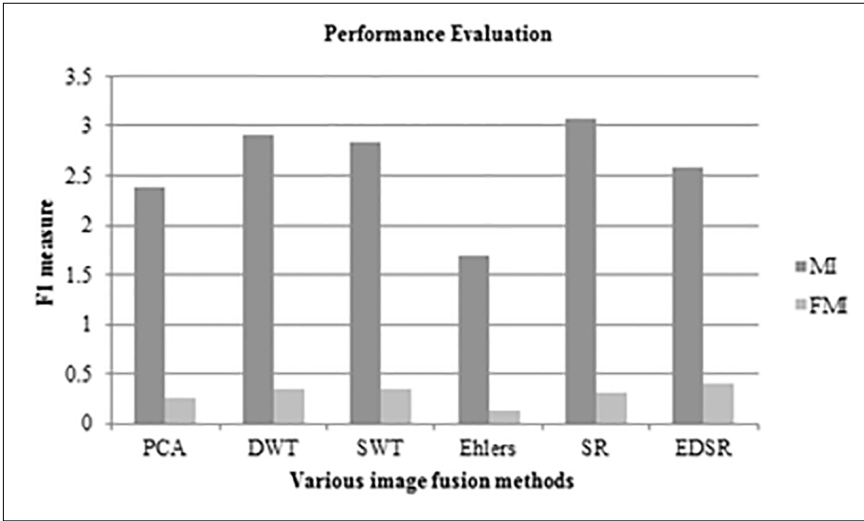


Figure 12 - Performance Evaluation with respect to MI and FMI for dataset 2.

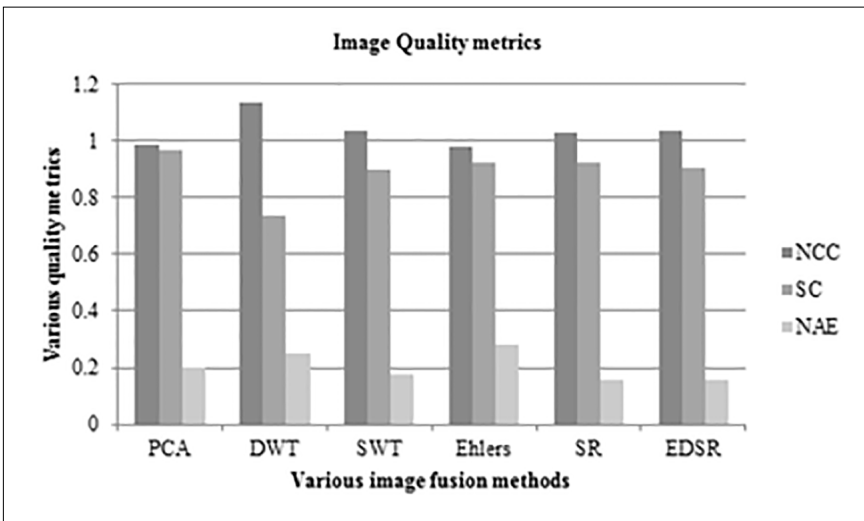


Figure 13 - Various image quality metrics for dataset 2.

Results from Table 1 and Figures 8, 9, and 10 show that the proposed EDSR has the lowest RMSE value of 20.40 and the highest MI of 3.47 and FMI of 0.48, as well as the best values for DD, UIQI, and ERGAS compared with PCA, DWT, SWT, Ehlers, and SR. The PSNR value of the EDSR is slightly lighter than DWT. The proposed EDSR has a lower NAE value of 0.11 and the highest SC value of 1.03 compared with the existing methods discussed above. These findings indicate that the EDSR outperforms SR, Ehlers, DWT, SWT, and PCA for dataset 1 in the fusion of multitemporal remote sensing images.

Results from Table 2 and Figures 11, 12, and 13 show that the proposed EDSR has the

lowest RMSE value of 20.19 and the highest PSNR value of 21.20 and FMI value of 0.40 compared with PCA, DWT, SWT, Ehlers, and SR. The MI value of the EDSR is slightly less than SR. The degree of distortion of the proposed method is less than the existing methods. Also, there is the highest UIQI value and the lowest ERGAS value compared with the existing methods, which proves the effectiveness of the EDSR method. The proposed EDSR has a lower NAE value of 0.15 than the existing methods discussed above. These findings indicate that the EDSR outperforms SR, Ehlers, DWT, SWT, and PCA for dataset 2 in the fusion of multitemporal remote sensing images. It is clear that the proposed EDSR provides better fused results naturally with a few disadvantages compared with the existing methods. The proposed method is more focused on remote sensing fusion, which can be used for further analysis.

The fusion results obtained using the different algorithms are shown in Figures 3, 4, 6, and 7. Visually, the proposed method performs competitively with other state-of-the-art methods. To better illustrate the difference of the fusion results, quantitative results are reported in Tables I and II, which show the RMSE, PSNR, MI, FMI, NCC, SC, NAE, DD, UIQI, and ERGAS for all methods. It can be seen that the proposed method always provides the best results compared with the existing methods.

Conclusion and future works

In this paper, a multitemporal-based remote sensing image fusion has been proposed based on an improved sparse coding and updating dictionary. The proposed method uses both the lower bound and the upper bound to construct the dictionary adaptively. The dictionary is learned from the source images for better robustness and effectiveness. It is observed that the regularization parameter is constant in the existing sparse, whereas the proposed method utilizes the regularization parameter adaptively and effectively. The proposed EDSR takes advantage of the adaptive regularization parameter and chooses the maximum absolute fused vectors for fusion. Thus, the EDSR performs better than the traditional methods and basic sparse representation fusion.

The various image fusion metrics evaluated show that the proposed EDSR technique outperforms all other existing methods in terms of various quality metrics such as RMSE, PSNR, MI, FMI, SC, NCC, NAE, DD, UIQI, and ERGAS. In the future, the proposed remote sensing image fusion technique can be applied to PAN and MS images.

References

- Aharon M., Elad M., Bruckstein A. (2006) - *K-SVD: An Algorithm for Designing Overcomplete Dictionaries for Sparse Representation*. IEEE Transactions on Signal Processing, 54 (11): 4311-4322. doi: <http://dx.doi.org/10.1109/TSP.2006.881199>.
- Aharon M. (2006) - *Overcomplete dictionaries for sparse representation of signals*. Ph.D. Thesis, Technion-Israel Institute of Technology, Faculty of Computer Science.
- Bach F., Mairal J., Ponce J., Sapiro G. (2010) - *Sparse coding and dictionary learning for image analysis*. Proceedings of IEEE International Conference on Computer Vision and Pattern Recognition, San Francisco.
- Bo H., Huihui H. (2012) - *Spatiotemporal reflectance fusion via sparse representation*. IEEE Transactions on Geoscience and Remote Sensing, 50 (10): 3707-3716. doi: <http://dx.doi.org/10.1109/TGRS.2012.2186638>.

- Du P., Liu S., Gamba P., Tan K., Xia J. (2012) - *Fusion of difference images for change detection over urban areas*. IEEE Journal of Selected Topics in Applied Earth Observations and Remote Sensing, 5 (4): 1076-1086. doi: <http://dx.doi.org/10.1109/JSTARS.2012.2200879>.
- Flusser J., Sroubek F., Barbara Zitova B. (2007) - *Image fusion: principles, methods, and applications*. Tutorial Eusipco.
- Gong M., Zhou Z., Ma J. (2012) - *Change detection in synthetic aperture radar images based on image fusion and fuzzy clustering*. IEEE Transactions on Image Processing, 21 (4): 2141-2151. doi: <http://dx.doi.org/10.1109/TIP.2011.2170702>.
- Haghighat M., Akbari B., Aghagolzadeh A., Seyedarabi H. (2011) - *A non-reference image fusion metric based on mutual information of image features*. Computers & Electrical Engineering, 37(5): 744-756. doi: <http://dx.doi.org/10.1016/j.compeleceng.2011.07.012>.
- Haghighat M., Razian M.A. (2014) - *Fast-FMI: non-reference image fusion metric*. International Conference on Application of Information and Communication Technologies (AICT), pp. 1-3. doi: <http://dx.doi.org/10.1109/icaict.2014.7036000>.
- He X., Condat L., Bioucas-Dias J.M., Chanussot J., Xia J. (2014) - *A new pansharpening method based on spatial and spectral sparsity priors*. IEEE Transactions on Image Processing, 23 (9): 4160-4174. doi: <http://dx.doi.org/10.1109/TIP.2014.2333661>.
- Jagalingam P., Hegde A.V. (2015) - *A Review of Quality Metrics for Fused Image*. Aquatic Procedia, 4: 133-142. doi: <http://dx.doi.org/10.1016/j.aqpro.2015.02.019>.
- Knee P. (2012) - *Sparse Representations for Radar with MATLAB® Examples*. Synthesis Lectures on Algorithms and Software in Engineering, 4 (1): 1-85. doi: <http://dx.doi.org/10.2200/S00445ED1V01Y201208ASE010>.
- Lal A.M., Anuncia S.M. (2015a) - *Detection of Boundaries by Fusing the Topographic Sheets and Multi-Spectral Images for Geographic Landscapes*. International Journal of Ecology & Development, 30 (3): 11-25.
- Lal A.M., Anuncia S.M. (2015b) - *Semi-supervised change detection approach combining sparse fusion and constrained k means for multi-temporal remote sensing images*. The Egyptian Journal of Remote Sensing and Space Science, 18: 279-288. doi: <http://dx.doi.org/10.1016/j.ejrs.2015.10.002>.
- Lal A.M., Anuncia S.M., Gopalakrishnan M. (2015a) - *Multispectral image change revealing using translation invariant wavelet transform fusion and adaptive K-means clustering*. International Journal of Applied Environmental Sciences, 10 (2): 681-693.
- Lal A.M., Anuncia S.M., Kombo O.H. (2015b) - *A Hybrid Approach for Fusion Combining SWT and Sparse Representation in Multispectral Images*. Indian Journal of Science and Technology, 8 (16). doi: <http://dx.doi.org/10.17485/ijst/2015/v8i16/66346>.
- Liu Y., Liu S., Wang Z. (2015) - *A general framework for image fusion based on multi-scale transform and sparse representation*. Information Fusion, 24: 147-164. doi: <http://dx.doi.org/10.1016/j.inffus.2014.09.004>.
- Lu X., Yuan H., Yan P., Li L., Li X. (2011) - *Image Denoising via Improved Sparse Coding*. In: BMVC 2011, The 22nd British Machine Vision Conference, University of Dundee, 29 August - 2 September 2011, pp. 1-11. doi: <http://dx.doi.org/10.5244/C.25.74>.
- Mahboob I., Chen J., Wen X.-Z., Li C.-S. (2012) - *Remote sensing image fusion using best bases sparse representation*. IEEE International Geoscience and Remote Sensing Symposium, 22-27 July 2012, Munich, pp. 5430-5433. doi: <http://dx.doi.org/10.1109/>

- IGARSS.2012.6352378.
- Pohl C. (2014) - *Challenges of remote sensing image fusion to optimize earth observation data exploitation*. European Scientific Journal, 4: 365-365.
- Sumathi M., Barani R. (2012) - *Qualitative evaluation of pixel level image fusion algorithms*. IEEE International Conference on Pattern Recognition, Informatics and Medical Engineering (PRIME), pp. 312-317. doi: <http://dx.doi.org/10.1109/ICPRIME.2012.6208364>.
- Sivasangamani S., Gomathi P.S., Kalaavathi B. (2014) - *Multimodal Medical Image Fusion using Neighbouring Pixel Selection*. International Journal of Bio-Science and Bio-Technology, 6 (3): 97-108. doi: <http://dx.doi.org/10.14257/ijbsbt.2014.6.3.12>.
- Tropp J.A., Gilbert A.C. (2007) - *Signal recovery from random measurements via orthogonal matching pursuit*. IEEE Transactions on Information Theory, 53 (12): 4655-4666. doi: <http://dx.doi.org/10.1109/TIT.2007.909108>.
- Vicinanza M.R., Restaino R., Vivone G., Dalla Mura M., Chanussot J. (2015) - *A Pansharpening Method Based on the Sparse Representation of Injected Details*. IEEE Geoscience and Remote Sensing Letters, 12 (1): 180-184. doi: <http://dx.doi.org/10.1109/LGRS.2014.2331291>.
- Wei Q., Bioucas-Dias J., Dobigeon N., Tourneret J.-Y. (2015) - *Hyperspectral and multispectral image fusion based on a sparse representation*. IEEE Transactions on Geoscience and Remote Sensing, 53 (7): 3658-3668. doi: <http://dx.doi.org/10.1109/TGRS.2014.2381272>.
- Wang Z., Ziou D., Armenakis C., Li D., Li Q. (2005) - *A comparative analysis of image fusion methods*. IEEE Transactions on Geoscience and Remote Sensing, 43 (6): 1391-1402. doi: <http://dx.doi.org/10.1109/TGRS.2005.846874>.
- Yang B., Li S. (2010) - *Multifocus image fusion and restoration with sparse representation*. IEEE Transactions on Instrumentation and Measurement, 59 (4): 884-892. doi: <http://dx.doi.org/10.1109/TIM.2009.2026612>.
- Yu X., Gao G., Xu J., Wang G. (2014) - *Remote sensing image fusion based on sparse representation*. IEEE International Geoscience and Remote Sensing Symposium (IGARSS), pp. 2858-2861.
- Zheng Y. (2011) - *Image fusion and its applications*. INTECH open access publisher.
- Zhu X.-X., Bamler R. (2013) - *A sparse image fusion algorithm with application to pansharpening*. IEEE Transactions on Geoscience and Remote Sensing, 51 (5): 2827-2836. doi: <http://dx.doi.org/10.1109/TGRS.2012.2213604>.

© 2016 by the authors; licensee Italian Society of Remote Sensing (AIT). This article is an open access article distributed under the terms and conditions of the Creative Commons Attribution license (<http://creativecommons.org/licenses/by/4.0/>).